Dynamic Analysis of a Brushless D.C. Motor Using a Modified Harmonic Balance Method

Ming-ran Lee

Chandramouli Padmanabhan
Graduate Research Associates.

Rajendra Singh
Professor.
Fellow ASME

Acoustics and Dynamics Laboratory,
Department of Mechanical Engineering,
The Ohio State University,
206 West 18th Avenue,
Columbus, OH 43210-1107

Analysis of brushless d.c. motor (BDCM) torque pulsations is an essential step in the diagnosis and control of vibration and noise generated by many electro-mechanical devices. The broad band spectral content of the torque pulsations, as predicted by a mathematical model which accounts for various complex effects, can often be obtained only by numerical integration which is time consuming while permitting little understanding of the dynamic interactions. Prior analytical approaches, such as the Fourier series technique or the d-q axis theory, are limited by the simplifying assumptions needed to compute the torque spectrum. This paper develops a new semi-analytical formulation for the analysis of nonlinear, time-varying BDCM's which involve both spatial and temporal domains. A modified multi-term harmonic balance method, based on a transformation of the dual-domain problem to a spatial domain formulation, is developed here specifically to compute the magnitude of several harmonics of the pulsating torque. The interacting effects of key parameters, like dynamic eccentricity, magnetic saturation and open stator slots, on the time-varying inductances and rotor flux density distribution are included explicitly in the formulation. The predicted spectra compare very well with those obtained by direct time domain numerical integration. Yet, the proposed method is computationally efficient especially when the model dimension is reduced. It also provides better insight into the high frequency dynamics of the sample case.

1 Introduction

The development of a mathematical model for brushless d.c. motors (BDCM) is an essential step in the study of the vibro-acoustic characteristics of many electro-mechanical devices such as cassette recorders, laser printers and computer disk drives. Of interest usually is the prediction of motor torque pulsations which may be the primary source of dynamic excitation. Conventional analyses of BDCM's are usually based on one of the three approaches (Bolton et al., 1986), namely the state-variable formulation (Pillay and Krishnan, 1989), the Fourier series representation (Bolton and Ashen, 1984) and the equivalent d-q axis model (Krause and Wasynczuk, 1989). Previous investigations have, however, focused mainly on the lower frequencies. The state variable model yields the time history of torque using any numerical integration scheme. Subsequently, the torque spectrum is obtained by applying an FFT algorithm to the steady-state time trace. The numerical integration is time consuming since very small integration steps are necessary to obtain accurate high frequency information of interest in predicting the torque spectrum. Though the Fourier series model is an analytical frequency domain formulation, several simplifying assumptions have to be made apriori in order to derive an explicit expression. For instance, the fluctuation of angular velocity has to be ignored, which may not be true for some cases, to ensure a tractable analytical formulation. The emphasis of this method is therefore on the frequency content rather than the magnitude of the torque spectrum. The *d-q* axis model, which can only be developed for a simple BDCM, is used primarily for the purpose of developing control strategies. It is obvious that all of these approaches are limited in their ability to predict the torque spectrum over a broad frequency range. An efficient analytical or semi-analytical formulation, capable of accurately predicting the torque spectrum over a wide frequency range, while incorporating relevant dynamic interaction effects, is clearly needed. Such a method may also lead to an improved understanding of various physical mechanisms and dynamic behavior, especially at higher frequencies.

The multi-term harmonic balance method (also referred to as the Galerkin's method) has been widely used in solving nonlinear dynamic equations (Urabe and Reiter, 1966; Chua and Ushida, 1981; Ushida and Chua, 1984; Ling and Wu, 1987). The scheme is quite powerful since it can handle a wide variety of nonlinearities, which may be weak or strong, smooth or piecewise continuous. Its ability to handle complex effects, coupled with the fact that solutions are obtained directly in the frequency domain, makes it more efficient than the direct numerical integration method. A general theory of the harmonic balance method for nonlinear dynamic equations has been developed in an earlier paper by Urabe and Reiter (1966). Generic formulations for both first and second-order systems were derived and several examples were solved using an iterative Newton-Raphson based technique. Ling and Wu (1987) increased the computational efficiency by employing the Broyden method and the Fast Fourier Transform (FFT) in the numerical scheme. The methodology was later extended to multi-frequency excitation problems, with incommensurable frequencies, by Chua and Ushida (1981) and Ushida and Chua (1984). Most of the applications of this technique, however, have been restricted to simple nonlinear electrical circuits or mechanical oscillators with a few degrees-of-freedom. A comprehensive study of electro-mechanical systems with time-varying (parametric) and nonlinear properties, is yet to be attempted. The focus of this paper is on the analysis of such systems, with a BDCM as the sample case. Also, the current paper is an extension of the BDCM theory presented recently by Lee and Singh (1992).

2 Problem Formulation

2.1 Scope and Objectives. The main objective of this study is to develop a steady-state spectral analysis scheme,

Contributed by the Dynamic Systems and Control Division for publication in the JOURNAL OF DYNAMIC SYSTEMS, MEASUREMENT, AND CONTROL. Manuscript received by the DSCD June 28, 1993. Associate Technical Editor: C. W. de Silva.

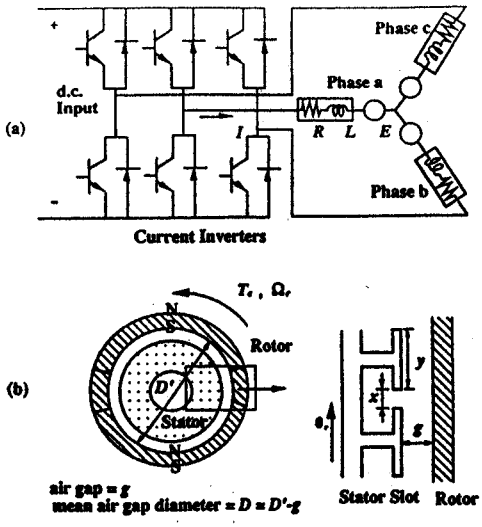

Fig. 1 Schematic of 3-phase 2-pole brushless d.c. motor

based on a modified multi-term harmonic balance method, for a nonlinear time-varying (NLTV) BDCM model. The model is essentially equivalent to three first-order electrical circuit equations with time-varying parameters and a first-order equation governing the mechanical system dynamics, arising due to the angular velocity fluctuations. Further, the model includes inductance and back e.m.f. harmonics associated with the dynamic eccentricity, open stator slots and magnetic saturation. The equations, which involve parameters that are functions of both spatial and temporal variables, are transformed to the spatial domain. The harmonic balance scheme is then applied to compute the magnitude of the torque spectrum. Next, the three phase equivalent circuit model is simplified to a single equivalent circuit by assuming a balanced phase relationship between the stator phase currents. Finally the mechanical system dynamics model is excluded from the original NLTV formulation, for analyzing cases where the angular velocity fluctuations may be negligible. These simplifications of the NLTV formulation are carried out intentionally, in order to understand the capabilities of the harmonic balance scheme, as well as to examine the effects of the various parameters on the resulting torque spectrum.

2.2 Brushless D.C. Motor Model. The derivation of the governing equations of a typical brushless d.c. motor consists of three parts: stator phases, electromechanical torque, and mechanical system dynamics. A typical 3-phase, 2-pole brushless d.c. motor is shown schematically in Fig. 1. The motor stator phases are represented in terms of equivalent electrical circuits; the voltage equation for each stator phase is expressed as:

$$v_k(t) = i_k(t)R + \frac{d\lambda_k}{dt} \tag{1}$$

where $i_k(t)$ is the phase current of the k-th stator phase, $v_k(t)$ is the line-to-neutral input voltage and R is the phase resistance. The flux linkage $\lambda_k(t)$ includes magnetizing flux linkages between the kth stator phase windings and the other stator phase windings and the permanent magnet on rotor. To simplify this problem, the coupled circuits are assumed to be linear magnetic systems without magnetic leakage, so that

$$\lambda_k(t) = \sum_j L_{kj}(\theta_r; t) i_j(t) + \lambda_{r,k}(t); \quad j = a, b, c \tag{2}$$

where $\lambda_{r,k}(t)$ is the flux linkage of the kth stator phase windings associated with the rotor permanent magnet, $L_{kj}(\theta_r; t)$ is the inductance of the kth stator phase with respect to the jth stator phase and θ_r is the angular position of the rotor. Since $d\lambda_{r,k}/dt$ is the induced voltage $e_k(t)$ in the kth stator phase (Pillay and Krishnan, 1989), the governing equation for the equivalent circuit of the kth stator phase is then written as:

$$v_k(t) = i_k(t)R + \sum_j \left(i_j(t) \frac{dL_{kj}(\theta_r; t)}{dt} + L_{kj}(\theta_r; t) \frac{di_j}{dt} \right) + e_k(t); \quad j = a, b, c \tag{3}$$

The voltage equations for all the stator phases can be given in matrix form:

$$\mathbf{V}(t) = \mathbf{R}\mathbf{I}(t) + \mathbf{L}(\theta_r; t)\left[\frac{d}{dt}\mathbf{I}\right] + \left[\frac{d}{dt}\mathbf{L}\right]\mathbf{I}(t) + \mathbf{E}(t) \tag{4}$$

For a three-phase BDCM,

$$\mathbf{E}(t) = [e_a(t) \quad e_b(t) \quad e_c(t)]^T;$$

$$\mathbf{V}(t) = [v_a(t) \quad v_b(t) \quad v_c(t)]^T$$

$$\mathbf{I}(t) = [i_a(t) \quad i_b(t) \quad i_c(t)]^T$$

$$\mathbf{L}(\theta_r; t) = \begin{bmatrix} L_{aa}(\theta_r; t) & L_{ab}(\theta_r; t) & L_{ac}(\theta_r; t) \\ L_{ba}(\theta_r; t) & L_{bb}(\theta_r; t) & L_{bc}(\theta_r; t) \\ L_{ca}(\theta_r; t) & L_{cb}(\theta_r; t) & L_{cc}(\theta_r; t) \end{bmatrix}$$

$$\mathbf{R} = \begin{bmatrix} R & 0 & 0 \\ 0 & R & 0 \\ 0 & 0 & R \end{bmatrix} \tag{5–9}$$

The back e.m.f. is proportional to the rotor flux density distribution, which can be approximated by a trapezoidal wave form (Bolton et al., 1986; Pillay and Krishnan, 1989). A more accurate model for the back e.m.f. can, however, be obtained by using a Fourier analysis (Boules, 1985), which is employed in this study. The stored energy $W(t)$ for a three-phase motor, in terms of the inductances and back e.m.f., is expressed as (Pillay and Krishnan, 1989)

$$W(t) = \left\{ \sum_k \int e_k i_k dt \right\} + \frac{1}{2}\left\{ \sum_{k,j} L_{kj}(\theta_r; t) i_k(t) i_j(t) \right\} \quad j, k = a, b, c \tag{10}$$

The electromechanical torque T_e is the derivative of the stored energy with respect to the rotor angular position $\theta_r = \int \Omega_r(\tau) d\tau$:

$$T_e(\theta_r; t) = \frac{1}{\Omega_r(t)} \mathbf{E}(t)^T \mathbf{I}(t) + \frac{1}{2} \mathbf{I}(t)^T \left[\frac{d}{d\theta_r} \mathbf{L}(\theta_r; t)\right] \mathbf{I}(t) \tag{11}$$

where $\Omega_r(t) = \bar{\Omega}_r + \tilde{\Omega}_r(t)$, is the total angular velocity of the rotor with $\bar{\Omega}_r$ representing the mean angular velocity and $\tilde{\Omega}_r(t)$ the fluctuating component. The torsional dynamics model of the mechanical system is given in terms of the mass moment of inertia of the motor J and a viscous damping coefficient B_m.

$$J \frac{d}{dt} \Omega_r(t) + B_m \Omega_r(t) = T_e(\theta_r; t) \tag{12}$$

Combining Eqs. (4), (11) and (12), one obtains the governing equations for a typical BDCM.

$$\mathbf{L}(\theta_r; t) \frac{d}{dt} \mathbf{I}(t) + \left[\frac{d}{dt} \mathbf{L}(\theta_r; t) + \mathbf{R}\right] \mathbf{I}(t) = \mathbf{V}(t) - \mathbf{E}(t) \tag{13}$$

$$J\frac{d}{dt}\Omega_r(t) + B_m\Omega_r(t)$$

$$= \frac{1}{\Omega_r(t)}\mathbf{E}(t)^T\mathbf{I}(t) + \frac{1}{2}\mathbf{I}(t)^T\left[\frac{d}{d\theta_r}\mathbf{L}(\theta_r; t)\right]\mathbf{I}(t) \quad (14)$$

2.3 Inductance Matrix and the Back E.M.F. Vector. If the airgap is uniform and there are no mechanical or electrical defects, the inductances can be assumed to be constant. The three-phase circuit equations, given by Eq. (4), can be reduced to a single equation by assuming balanced stator phase variables. Also the torque from Eq. (11) will include only the first term. However, in this study, variations of inductance associated with several mechanical and electrical effects are included since they influence the high frequency dynamics.

The dynamic eccentricity (Yang, 1981; Cameron et al., 1986), open stator slots (Yang, 1981; Bolton et al., 1986; Jufer, 1987), and magnetic saturation (Jufer, 1987) are key factors influencing motor torque pulsations. Prior studies have focused primarily on a single parameter effect (Cameron et al., 1986; Jufer, 1987) or only on the frequency content (Yang, 1981). Since a complete study of the combined effects of all parameters on a BDCM is not available in the literature, these are analytically incorporated into the BDCM model by including the variation of permeance associated with each parameter or cause. The Fourier series of the rotor flux density is multiplied by the permeance wave forms associated with dynamic eccentricity and open stator slots, which are also represented in terms of Fourier series, so that

$$B(\theta_r) = \sum_{\text{odd } q}^{\infty}\sum_{m=1}^{\infty}\sum_{n=1}^{\infty} K_{B,qN_P/2}K_{e,m}K_{S,N_s,n} \times \cos\left[\frac{qN_P}{2}\theta_r\right]\cos\left[m\theta_r\right]\cos\left(nN_s\theta_r\right) \quad (15)$$

where N_P is the number of rotor magnetic poles and N_s is the number of stator slots, K_B is the Fourier coefficient of rotor flux density distribution for a uniform air gap; K_e and K_S are Fourier coefficients associated with the dynamic eccentricity and open stator slots. For a concentrated stator winding, one obtains the back e.m.f. for stator phase a (see Bolton et al., 1986) as

$$e_a(\theta_r; t) = \Omega_r(t)N_wDlB(\theta_r) = \Omega_r(t)\hat{e}_a(\theta_r) \quad (16)$$

where N_w is the number of turns of stator phase windings, D is the mean airgap diameter and l is the length of rotor. The back e.m.f. for other stator phases are obtained by assuming a balanced phase relationship:

$$e_b(\theta_r; t) = e_a\left(\theta_r - \frac{4\pi}{3N_P}; t\right);$$

$$e_c(\theta_r; t) = e_a\left(\theta_r + \frac{4\pi}{3N_P}; t\right)$$

The line-to-neutral phase voltage wave form, $\mathbf{V}(t)$, is a quasi-square type and the same phase relationship is assumed for all three stator phases. In a practical situation, the voltage wave form will be of square-wave shape, but it will be chopped in a PWM fashion to provide constant current drive-consequently, the wave form will have higher frequency components at the PWM switching frequencies. Self and mutual inductances, as described below, include variations associated with the dynamic eccentricity and magnetic saturation.

$$L_{aa}(\theta_r) = \bar{L}[1 + \sum_{q=1}^{\infty}\sum_{s=1}^{\infty} K_{E,qN_P}K_{e,s}\cos\left(qN_P\theta_r\right)\cos\left(s\theta_r\right)] \quad (19)$$

$$L_{bc}(\theta_r) = \bar{M}[1 + \sum_{q=1}^{\infty}\sum_{s=1}^{\infty} K_{E,qN_P}K_{e,s}\cos\left(qN_P\theta_r\right)\cos\left(s\theta_r\right)] \quad (20)$$

Table 1 Harmonic groups

Parameter/variable	Harmonic groups
Eccentricity	$k\Omega_r$; $k = 1, 2, 3, \cdots$
Magnetic saturation	$kN_P\Omega_r$
Open stator slot	$kN_s\Omega_r$
Inductance	$(N_Pk_1 \pm k_2)\Omega_r$; $k_1, k_2, \in [0, 3]$
Phase voltage	$\frac{N_P}{2}(2k-1)\Omega_r$
Back e.m.f.	$\left[\frac{N_P}{2}(2k_1-1) \pm N_sk_2 \pm k_3\right]\Omega_r$; $k_1 \in [1, 13]$; $k_2, k_3 \in [0, 3]$
Phase current	$\left[\frac{N_P}{2}(2k_1-1) \pm N_sk_2 \pm N_Pk_3 \pm k_4\right]\Omega_r$; $k_1 \in [1, 13]$; $k_2, k_3, k_4 \in [0, 3]$
Rotor angular velocity and Torque	$[N_Pk_1 \pm N_sk_2 \pm N_Pk_3 \pm k_4]\Omega_r$; $k_1 \in [1, 13]$; $k_2, k_3, k_4 \in [0, 3]$

where K_E is the Fourier coefficient associated with magnetic saturation, and $\bar{L}$ and $\bar{M}$ are mean values of self and mutual inductances. Other components are obtained by assuming a phase relationship as shown below (see Lee and Singh, 1992):

$$L_{bb}(\theta_r) = L_{aa}\left(\theta_r - \frac{4\pi}{3N_P}\right);$$

$$L_{cc}(\theta_r) = L_{aa}\left(\theta_r + \frac{4\pi}{3N_P}\right) \quad (21, 22)$$

$$L_{ca}(\theta_r) = L_{bc}\left(\theta_r - \frac{4\pi}{3N_P}\right);$$

$$L_{ab}(\theta_r) = L_{bc}\left(\theta_r + \frac{4\pi}{3N_P}\right) \quad (23, 24)$$

3 The Modified Harmonic Balance Method

In the previous section, the electromechanical model of the BDCM, accounting for various effects, was developed. Each effect was represented by a trigonometric series, composed of a family of harmonics of the rotor angular position, θ_r, or combinations of several harmonic families. Table 1 summarizes the various harmonic groups involved in the formulation. The frequency contents of the harmonic families have been validated by comparison with measured radiated noise data (Lee and Singh, 1992).

The harmonic balance method essentially assumes a truncated trigonometric series for the steady-state solution of the state-space variables. The frequencies included in the series, therefore, must consist of all the harmonic families of Table 1 as well as their intermodulation components. Unlike most of the simple electrical circuit or mechanical oscillator problems solved earlier in the literature, the fundamental excitation frequency is not a constant. However, the concept of spatial periodicity of the rotor angular position ($\theta_r \in [0, 2\pi]$) is exploited in the formulation developed. This modified formulation then leads to a compact semi-analytical solution methodology which may be used to examine the influence of each parameter in a very efficient manner as opposed to direct time domain numerical integration.

The proposed methodology for the computation of the coefficients of the trigonometric series, representing the state-space variables, is outlined below specifically for a BDCM model:

1 Represent the state-space variables as well as the various parameter effects in terms of truncated trigonometric series expansions of the rotor angular position θ_r. The coefficients of the trigonometric series, representing the pa-

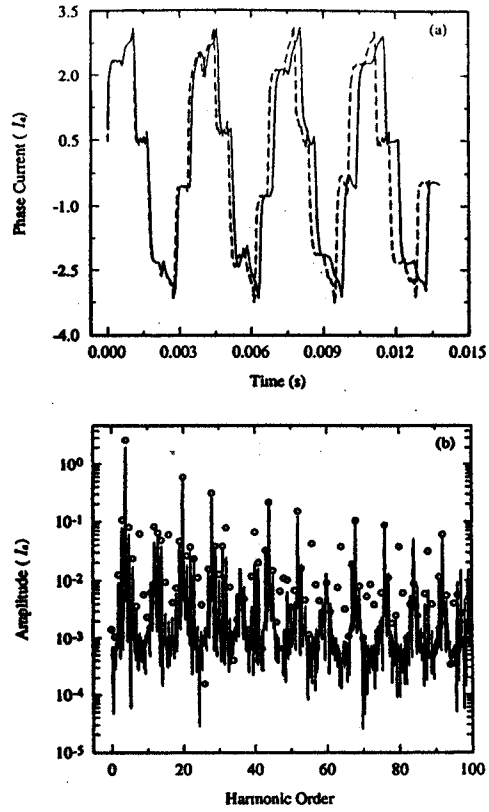

Fig. 2 Steady-state phase current of the NLTV model; (a) time domain, (b) frequency domain. Key: solid line: the numerical integration, dashed line and circles: the modified harmonic balance method.

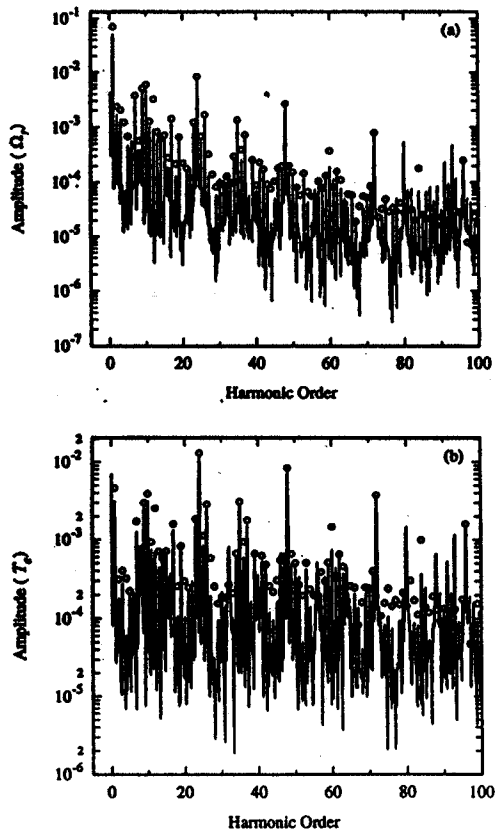

Fig. 3 Steady-state spectra of the NLTV model; (a) rotor angular velocity, (b) torque. Key: solid line: the numerical integration, circles: the modified harmonic balance method.

rameter effects, are implicit functions of the unknown coefficients of the state-space variables.

2 Substitute these expressions in the governing equations leading to nonlinear algebraic equations in terms of the unknown trigonometric coefficients of the state variables.

3 These equations hold for all values of θ_r, but in order to reduce the computation involved, the algebraic equations are assumed to hold only at selected discrete rotor angular positions (collocation). This step leads to the formation of the trigonometric collocation or Discrete Fourier Transform (DFT) matrices, $\mathbf{T}$ and $\mathbf{T}_v$, which are defined in Section 4.

4 The numerical computation is started by assuming initial values for the state-space variables' coefficients. The parameter coefficients are obtained from these by means of an IDFT (Inverse Discrete Fourier Transform) followed by a DFT. These are then used in the evaluation of the nonlinear algebraic equations.

5 Finally, the corrections for the unknown coefficients' values are obtained from a Newton-Raphson iterative scheme, which requires the construction and evaluation of a Jacobian matrix. The entire procedure outlined in steps 3 and 4 is repeated until the coefficient values converge and the truncation error involved is sufficiently small.

4 Nonlinear Time Varying (NLTV) Model

The BDCM is essentially a dual-domain (rotor angular position and time) problem, as evident from Eqs. (13) and (14). Unlike typical nonlinear systems studied before, the mean excitation frequency, $\bar{\Omega}_r$, in a BDCM model is also unknown. The collocation matrices, $\mathbf{T}$ and $\mathbf{T}_v$, would change every iteration, if the state variables were to be expressed in the time domain. Therefore, a spatial domain representation is used to represent the phase currents and angular velocity. This ensures that the normalized period will be 2π. The governing equations in the spatial domain are as follows, where $(\ )'$ denotes derivative with respect to θ_r:

$$\Omega_r(\theta_r)\mathbf{L}(\theta_r)\mathbf{I}'(\theta_r) + [\Omega_r(\theta_r)\mathbf{L}'(\theta_r) + \mathbf{R}]\mathbf{I}(\theta_r) = \mathbf{V}(\theta_r) - \Omega_r(\theta_r)\hat{\mathbf{E}}(\theta_r) \quad (25)$$

$$J\Omega_r(\theta_r)\Omega_r'(\theta_r) + B_m\Omega_r(\theta_r) = \hat{\mathbf{E}}^T(\theta_r)\mathbf{I}(\theta_r) + \tfrac{1}{2}\mathbf{I}^T(\theta_r)\mathbf{L}'(\theta_r)\mathbf{I}(\theta_r) \quad (26)$$

where $\mathbf{E}(\theta_r; t) = \Omega_r(\theta_r; t)\hat{\mathbf{E}}(\theta_r)$ (see Eq. (16)). In most cases, $\bar{\Omega}_r$ of the rotor is much larger than the fluctuating term, $\tilde{\Omega}_r(t)$. Consequently, the fundamental harmonic frequency of the torque pulsations is assumed to be $\bar{\Omega}_r$ which is then normalized to 1 in the spatial domain. The unknown steady-state currents and the angular velocity are thus expressed in terms of truncated trigonometric series, in the spatial domain, as follows.

Table 2 Predictions of mean rotor angular velocity

	$\bar{\Omega}_r/2\pi$ (Hz)		
		Harmonic balance method	
Harmonic groups included	Numerical integration	Full NLTV model	Reduced NLTV model
Eccentricity, saturation and open stator slots	72.0	74.5	75.0
Eccentricity	75.3	77.9	75.8
Saturation	74.0	76.8	77.2
Open stator slots	75.7	78.4	79.0

$$\mathbf{I}(\theta_r) = \mathbf{K}_{I,0} + \sum_{s=1}^{N} \mathbf{K}_{I,2s-1} \sin(f_s\theta_r) + \mathbf{K}_{I,2s} \cos(f_s\theta_r) \quad (27)$$

$$\Omega_r(\theta_r) = K_{\omega,0} + \sum_{s=1}^{N} K_{\omega,2s-1} \sin(f_s\theta_r) + K_{\omega,2s} \cos(f_s\theta_r) \quad (28)$$

Note that phase current and angular velocity could have different families of harmonic frequencies. This means that the dimensions of collocation matrices for the phase current and angular velocity will not be the same. To avoid this complexity, all harmonics of the fundamental frequency are included; that would be the case for the example solved, if all effects were to be included. The Fourier coefficient vector of size $4(2N + 1)$, is defined as:

$$\mathbf{K}_x = [K_{Ia,0} \quad \ldots \quad K_{Ia,2N+1} \quad K_{Ib,0} \quad \ldots \times K_{Ic,2N+1} \quad K_{\omega,0} \quad \ldots \quad K_{\omega,2N+1}]^T \quad (29)$$

Further, the various terms in equation (25) are expanded into individual trigonometric series as shown below:

$$\Omega_r \mathbf{L}\mathbf{I}' = \Gamma_1(\theta_r); \quad \{\Omega_r \mathbf{L}' + \mathbf{R}\}\mathbf{I} = \Gamma_2(\theta_r); \quad \Omega_r \hat{\mathbf{E}} = \Gamma_3(\theta_r) \quad (30\text{–}32)$$

$$\Gamma_i(\theta_r) = \gamma_{i,0} + \sum_{n=1}^{N} \{\gamma_{i,2n} \cos(f_n\theta_r) + \gamma_{i,2n-1} \sin(f_n\theta_r)\}; \quad i = 1, 2, 3 \quad (33)$$

$$\Gamma_i(\theta_r) = [\Gamma_{ia}(\theta_r) \quad \Gamma_{ib}(\theta_r) \quad \Gamma_{ic}(\theta_r)]^T; \quad \gamma_i = [\gamma_{ia}\gamma_{ib}\gamma_{ic}]^T; \quad i = 1, 2, 3 \quad (34, 35)$$

The terms in equation (26) are each similarly expanded into a trigonometric series:

$$J\Omega_r\Omega_r' = \Lambda_1(\theta_r); \quad B_m\Omega_r = \Lambda_2(\theta_r); \quad \hat{\mathbf{E}}\mathbf{I} = \Lambda_3(\theta_r); \quad \tfrac{1}{2}\mathbf{I}^T\mathbf{L}'\mathbf{I} = \Lambda_4(\theta_r) \quad (36\text{–}39)$$

$$\Lambda_i(\theta_r) = \alpha_{i,o} + \sum_{n=1}^{N} \{\alpha_{i,2n} \cos(f_n\theta_r) + \alpha_{i,2n-1} \sin(f_n\theta_r)\} \quad i = 1, \ldots, 4 \quad (40)$$

Note that $\mathbf{V}(\theta_r)$ and $\hat{\mathbf{E}}(\theta_r)$ are also written in terms of a Fourier series, with harmonic indices f_n of Table 1. An arrangement of coefficients of like terms on both sides of equations (25) and (26) corresponding to the harmonic index f_n yields $4(2N + 1)$ equations.

$$R_{s,n} \equiv K_{Vs,n} + \gamma_{3s,n} - \gamma_{1s,n} - \gamma_{2s,n} = 0; \quad s = a, b, c \quad n = 0, 1, \ldots, 2N$$

$$N_n \equiv \alpha_{3,n} + \alpha_{4,n} - \alpha_{1,n} - \alpha_{2,n} = 0 \quad (41, 42)$$

The corresponding functions represented by coefficients $R_{s,n}$ and N_n are defined by $R_s(\theta_r)$ and $N(\theta_r)$. Since the terms γ_n and α_n in Eqs. (41) and (42) are implicit functions of phase current coefficients $K_{Is,n}$ or angular velocity coefficients $K_{\omega,n}$ the above algebraic equations are nonlinear. Hence, an iterative Newton-Raphson method is employed to solve them, as shown below:

$$\mathbf{J}\{\Delta\mathbf{K}_x\} = \mathbf{Z} \quad (43)$$

where $\mathbf{J}$ is the Jacobian matrix and $\mathbf{Z}$ is a function of $\mathbf{K}_x$ and is defined by

$$\mathbf{Z} = [R_{a,0} \quad \ldots \quad R_{a,2N} \quad R_{b,0} \quad \ldots \quad R_{b,2N} \times R_{c,0} \quad \ldots \quad R_{c,2N} \quad N_0 \quad \ldots \quad N_{2N}]^T \quad (44)$$

The procedure is initiated by assuming a set of trial values for $\mathbf{K}_x$. The current vector $\mathbf{I}$ and rotor angular velocity Ω_r are sampled M times in the θ_r domain over $[0, 2\pi]$, where M is chosen such that spectral aliasing is avoided ($M \geq 2f_N$). This leads to a rectangular collocation matrix $\mathbf{T}$ of dimension M by $(2N + 1)$, as shown below:

$$T_{i,1} = 1; \quad T_{i,2j-1} = \sin(f_j\theta_{r,i}); \quad T_{i,2j} = \cos(f_j\theta_{r,i}) \quad (45a\text{–}c)$$

$$\theta_{r,i} = \frac{2\pi(i-1)}{M}; \quad i = 1, \ldots, M; \quad j = 1, \ldots, N; \quad (46)$$

The phase currents at evenly divided rotor positions are given by

$$[I_s(\theta_{r,1})\, I_s(\theta_{r,2}) \quad \ldots \quad I_s(\theta_{r,M})]^T = \mathbf{T}[K_{I,0}^s K_{I,1}^s \quad \ldots \quad K_{I,2N}^s]^T; \quad s = a, b, c \quad (47)$$

Similarly, the derivative of the phase currents with respect to θ_r can be expressed as

$$[I_s'(\theta_{r,1})\, I_s'(\theta_{r,2}) \cdots I_s'(\theta_{r,M})]^T = \mathbf{T}_v[K_{I,0}^s K_{I,1}^s \cdots K_{I,2N}^s]^T; \quad s = a, b, c \quad (48)$$

$$T_{vi,1} = 0; \quad T_{vi,2j-1} = f_j \cos(f_j\theta_{r,i}); \quad T_{vi,2j} = -f_j \sin(f_j\theta_{r,i}) \quad (49a\text{–}c)$$

The rotor angular velocity and its derivative at evenly divided rotor positions are expressed in a similar fashion. Further, $\mathcal{R}_s(\theta_r)$ and $\mathcal{N}(\theta_r)$ are given by:

$$\begin{bmatrix} \mathcal{R}_s(\theta_{r,1}) \\ \vdots \\ \mathcal{R}_s(\theta_{r,M}) \end{bmatrix} = \mathbf{T} \begin{bmatrix} \mathcal{R}_{s,0} \\ \vdots \\ \mathcal{R}_{s,2N} \end{bmatrix}; \quad \begin{bmatrix} \mathcal{N}(\theta_{r,1}) \\ \vdots \\ \mathcal{N}(\theta_{r,M}) \end{bmatrix} = \mathbf{T} \begin{bmatrix} \mathcal{N}_0 \\ \vdots \\ \mathcal{N}_{2N} \end{bmatrix}; \quad s = a, b, c \quad (50, 51)$$

From the above equations one can obtain $\mathcal{R}_{s,n}$ and $\mathcal{N}_n$ as follows:

$$\begin{bmatrix} \mathcal{R}_{s,0} \\ \vdots \\ \mathcal{R}_{s,2N} \end{bmatrix} = \{\mathbf{T}^T\mathbf{T}\}^{-1}\mathbf{T}^T \begin{bmatrix} \mathcal{R}_s(\theta_{r,1}) \\ \vdots \\ \mathcal{R}_s(\theta_{r,M}) \end{bmatrix};$$

$$\begin{bmatrix} \mathcal{N}_0 \\ \vdots \\ \mathcal{N}_{2N} \end{bmatrix} = \{\mathbf{T}^T\mathbf{T}\}^{-1}\mathbf{T}^T \begin{bmatrix} \mathcal{N}(\theta_{r,1}) \\ \vdots \\ \mathcal{N}(\theta_{r,M}) \end{bmatrix}; \quad s = a, b, c \quad (52, 53)$$

The Jacobian matrix $\mathbf{J}$, of dimension $4(2N + 1)$ by $4(2N + 1)$ in this case, is partitioned into 4 by 4 sub-matrices as

$$\mathbf{J} = \begin{bmatrix} \mathbf{J}^{aa} & \mathbf{J}^{ab} & \mathbf{J}^{ac} & \mathbf{J}^{a\Omega} \\ \mathbf{J}^{ba} & \mathbf{J}^{bb} & \mathbf{J}^{bc} & \mathbf{J}^{b\Omega} \\ \mathbf{J}^{ca} & \mathbf{J}^{cb} & \mathbf{J}^{cc} & \mathbf{J}^{c\Omega} \\ \mathbf{J}^{\Omega a} & \mathbf{J}^{\Omega b} & \mathbf{J}^{\Omega c} & \mathbf{J}^{\Omega\Omega} \end{bmatrix} \quad (54)$$

The elements J_{mn}^{sq} in each sub-matrix are defined by

$$J_{mn}^{sq} = \begin{cases} \dfrac{\partial \mathcal{R}_{s,m}}{\partial K_{Iq,n}} = -\dfrac{\Gamma_{1s,m}}{\partial K_{Iq,n}} - \dfrac{\Gamma_{2s,m}}{\partial K_{Iq,n}} & s, q = a, b, c \\ \dfrac{\partial \mathcal{R}_{s,m}}{\partial K_{\omega,n}} = \dfrac{\Gamma_{3s,m}}{\partial K_{\omega,n}} - \dfrac{\Gamma_{1s,m}}{\partial K_{\omega,n}} - \dfrac{\Gamma_{2s,m}}{\partial K_{\omega,n}} & s = a, b, c; q = \Omega \\ \dfrac{\partial \mathcal{N}_m}{\partial K_{Iq,n}} = \dfrac{\Lambda_{3s,m}}{\partial K_{Iq,n}} + \dfrac{\Lambda_{4s,m}}{\partial K_{Iq,n}} & s = \Omega; q = a, b, c \\ \dfrac{\partial \mathcal{N}_m}{\partial K_{\omega,n}} = -\dfrac{\Lambda_{1s,m}}{\partial K_{\omega,n}} - \dfrac{\Lambda_{2s,m}}{\partial K_{\omega,n}} & s, q = \Omega \end{cases} \quad (55)$$

To determine each term in the above equation, the following procedure needs to be adopted. Taking derivative of Eqs. (52) and (53) on both sides with respect to θ_r, one obtains

$$\frac{\partial}{\partial\theta_r}\left\{\begin{bmatrix}K_{Vs,0}\\ \vdots\\ K_{Vs,2N}\end{bmatrix}+\begin{bmatrix}\gamma_{3s,0}\\ \vdots\\ \gamma_{3s,2N}\end{bmatrix}-\begin{bmatrix}\gamma_{1s,0}\\ \vdots\\ \gamma_{1s,2N}\end{bmatrix}-\begin{bmatrix}\gamma_{2s,0}\\ \vdots\\ \gamma_{2s,2N}\end{bmatrix}\right\}$$

$$=\{\mathbf{T}^T\mathbf{T}\}^{-1}\mathbf{T}^T\frac{\partial}{\partial\theta_r}\begin{bmatrix}\mathcal{R}_s(\theta_{r,1})\\ \vdots\\ \mathcal{R}_s(\theta_{r,M})\end{bmatrix} \quad (56)$$

$$\frac{\partial}{\partial\theta_r}\left\{\begin{bmatrix}\alpha_{4,0}\\ \vdots\\ \alpha_{4,2N}\end{bmatrix}+\begin{bmatrix}\alpha_{3,0}\\ \vdots\\ \alpha_{3,2N}\end{bmatrix}-\begin{bmatrix}\alpha_{1,0}\\ \vdots\\ \alpha_{1,2N}\end{bmatrix}-\begin{bmatrix}\alpha_{2,0}\\ \vdots\\ \alpha_{2,2N}\end{bmatrix}\right\}$$

$$=\{\mathbf{T}^T\mathbf{T}\}^{-1}\mathbf{T}^T\frac{\partial}{\partial\theta_r}\begin{bmatrix}\mathcal{N}(\theta_{r,1})\\ \vdots\\ \mathcal{N}(\theta_{r,M})\end{bmatrix} \quad (57)$$

From Eq. (25) one can see that

$$\left.\frac{\partial\mathcal{R}_s(\theta_r)}{\partial K_{Iq,n}}\right|_{\theta_r=\theta_{r,k}}=-\frac{\partial}{\partial I'_q}\Big[\sum_{m=a,b,c}\Omega_r L_{sm}I'_m\Big]\left.\frac{\partial I'_q(\theta_r)}{\partial K_{Iq,n}}\right|_{\theta_r=\theta_{r,k}}$$
$$-\frac{\partial}{\partial I_q}\Big[\sum_{m=a,b,c}(\Omega_r L'_{sm}+R\delta_{sm})I_m\Big]\left.\frac{\partial I_q(\theta_r)}{\partial K_{Iq,n}}\right|_{\theta_r=\theta_{r,k}} \quad (58)$$

$$\left.\frac{\partial\mathcal{R}_s(\theta_r)}{\partial K_{\omega,n}}\right|_{\theta_r=\theta_{r,k}}=\frac{\partial}{\partial\Omega_r}\Big[\Omega_r\hat{E}_s-\Omega_r\sum_{m=a,b,c}(L'_{sm}I_m$$
$$+R\delta_{sm}I_m+L_{sm}I'_m)\Big]\left.\frac{\partial\Omega_r(\theta_r)}{\partial K_{\omega,n}}\right|_{\theta_r=\theta_{r,k}} \quad (59)$$

Expressing them in the matrix form and incorporating the collocation matrices, we have

$$\begin{bmatrix}\left.\frac{\partial\mathcal{R}_s(\theta_r)}{\partial K_{Iq,0}}\right|_{\theta_{r,1}} & \left.\frac{\partial\mathcal{R}_s(\theta_r)}{\partial K_{Iq,1}}\right|_{\theta_{r,1}} & \cdots & \left.\frac{\partial\mathcal{R}_s(\theta_r)}{\partial K_{Iq,2N}}\right|_{\theta_{r,1}}\\ \vdots & \ddots & & \vdots\\ \vdots & \vdots & \ddots & \vdots\\ \left.\frac{\partial\mathcal{R}_s(\theta_r)}{\partial K_{Iq,0}}\right|_{\theta_{r,M}} & \left.\frac{\partial\mathcal{R}_s(\theta_r)}{\partial K_{Iq,1}}\right|_{\theta_{r,M}} & \cdots & \left.\frac{\partial\mathcal{R}_s(\theta_r)}{\partial K_{Iq,2N}}\right|_{\theta_{r,M}}\end{bmatrix}$$
$$=\mathbf{Q}^1_{sq}\mathbf{T}_v+\mathbf{Q}^2_{sq}\mathbf{T}$$

$$\mathbf{Q}^1_{sq}=\mathrm{DIAG}[\Omega_r(\theta_{r,1})L_{sq}(\theta_{r,1})\quad\Omega_r(\theta_{r,2})L_{sq}(\theta_{r,2})$$
$$\ddots\qquad\qquad\cdots\quad\Omega_r(\theta_{r,M})L_{sq}(\theta_{r,M})]$$

$$\mathbf{Q}^2_{sq}=[\mathrm{DIAG}[\Omega_r(\theta_{r,1})L'_{sq}(\theta_{r,1})+\delta_{sq}R$$
$$\times\Omega_r(\theta_{r,2})L'_{sq}(\theta_{r,2})+\delta_{sq}R$$
$$\cdots\quad\Omega_r(\theta_{r,M})L'_{sq}(\theta_{r,M})+\delta_{sq}R] \quad (60a\text{–}c)$$

By incorporating Eq. (52) into Eq. (60), we obtain the following equation.

$$\mathbf{J}^{sq}=\begin{bmatrix}\frac{\partial\mathcal{R}_{s,0}}{\partial K_{Iq,0}} & \frac{\partial\mathcal{R}_{s,0}}{\partial K_{Iq,1}} & \cdots & \frac{\partial\mathcal{R}_{s,0}}{\partial K_{Iq,2N}}\\ \frac{\partial\mathcal{R}_{s,1}}{\partial K_{Iq,0}} & \frac{\partial\mathcal{R}_{s,1}}{\partial K_{Iq,1}} & \cdots & \frac{\partial\mathcal{R}_{s,1}}{\partial K_{Iq,2N}}\\ \vdots & \vdots & \ddots & \vdots\\ \frac{\partial\mathcal{R}_{s,2N}}{\partial K_{Iq,0}} & \frac{\partial\mathcal{R}_{s,2N}}{\partial K_{Iq,1}} & \cdots & \frac{\partial\mathcal{R}_{s,2N}}{\partial K_{Iq,2N}}\end{bmatrix}$$
$$=\{\mathbf{T}^T\mathbf{T}\}^{-1}\mathbf{T}^T\{\mathbf{Q}^1_{sq}\mathbf{T}_v+\mathbf{Q}^2_{sq}\mathbf{T}\};\quad s,q=a,b,c \quad (61)$$

Other sub-matrices of the Jacobian matrix are obtained similarly as:

$$\mathbf{J}^{sq}=\begin{cases}\{\mathbf{T}^T\mathbf{T}\}^{-1}\mathbf{T}^T\mathbf{Q}^3_s\mathbf{T} & \text{for } s=a,b,c;\ q=\Omega\\ \{\mathbf{T}^T\mathbf{T}\}^{-1}\mathbf{T}^T\mathbf{Q}^4_q\mathbf{T} & \text{for } s=\Omega;\ q=a,b,c\\ \{\mathbf{T}^T\mathbf{T}\}^{-1}\mathbf{T}^T\{\mathbf{Q}^5\mathbf{T}+\mathbf{Q}^6\mathbf{T}_v\} & \text{for } s,q=\Omega\end{cases}$$

$$\mathbf{Q}^3_s=\mathrm{DIAG}[\sum_{k=a,b,c}\{I_s(\theta_1)L_{sk}(\theta_1)\}'+\hat{E}_s(\theta_1)$$
$$\cdots\quad\sum_{k=a,b,c}\{I_s(\theta_M)L_{sk}(\theta_M)\}'+\hat{E}_s(\theta_M)]$$

$$\mathbf{Q}^4_q=\mathrm{DIAG}[-\sum_{k=a,b,c}I_k(\theta_1)L'_{qk}(\theta_1)-\hat{E}_q(\theta_1)$$
$$\cdots\quad-\sum_{k=a,b,c}I_k(\theta_M)L'_{qk}(\theta_M)-\hat{E}_q(\theta_M)]$$

$$\mathbf{Q}^5=\mathrm{DIAG}[J\Omega'_r(\theta_1)+B_m\quad\cdots\quad J\Omega'_r(\theta_M)+B_m]$$
$$\mathbf{Q}^6=\mathrm{DIAG}[J\Omega_r(\theta_1)\quad\cdots\quad J\Omega_r(\theta_M)] \quad (62a\text{–}g)$$

where DIAG denotes a diagonal matrix. Since the Jacobian matrix is a function of the phase currents and rotor angular velocity, it must be evaluated before every iteration. If a large number of harmonics are included, it would take a very long time to complete. Figures 2 and 3 compare results obtained from the modified harmonic balance method with those from numerical integration. It can be seen from Fig. 2(a) that there is a slight difference in Ω_r predicted by the two methods. Further, the phase currents are observed to be almost balanced, although the results are not shown here. Table 2 lists the corresponding mean angular velocity values when eccentricity, open stator slot and saturation effects are each considered individually as well as together. From the table it is clear that the error in the mean rotor speed between numerical integration and the harmonic balance scheme is rather small. Further, the harmonic amplitudes predicted by the modified harmonic balance method match well with numerical integration especially at the dominant harmonics, as evident from Figs. 2(b) and 3. Still, some of the harmonics over the higher frequency range show discrepancies, which are probably due to intrinsic numerical damping of the numerical integration scheme as well as errors associated with the Gibbs' effect caused by the piecewise continuous phase voltage.

5 Reduced NLTV Model

The modified harmonic balance method, for the NLTV BDCM model of Section 4, involves the computation of a Jacobian matrix of dimension 4 by $(2N+1)$. To evaluate a large number of harmonics, such as 100 used in the sample case, the computing time is enormous. Since the phase currents of the three stator phases obtained from the NLTV formulation are almost balanced (which implies that the three stator phase currents have the same wave form with a phase shift of $4\pi/3N_p$) their governing equations can be reduced to a single first order equivalent electrical circuit. This yields a Jacobian matrix of reduced size and consequently the computing time is less. The governing equations for the reduced model, which still includes the mechanical system dynamics, are:

$$[L_{aa}\Omega_r I'_a+L_{ab}\Omega_r I'_b+L_{ac}\Omega_r I'_c]$$
$$+[(L'_{aa}\Omega_r+R)I_a+L'_{ab}\Omega_r I_b+L'_{ac}\Omega_r I_c]=V_a-\Omega_r\hat{E}_a \quad (63)$$

$$J\Omega_r\Omega'_r+B_m\Omega_r=\hat{\mathbf{E}}^T\mathbf{I}+\tfrac{1}{2}\mathbf{I}^T\mathbf{L}'\mathbf{I} \quad (64)$$

$$i_b(\theta_r)=i_a\left(\theta_r-\frac{4\pi}{3N_P}\right);\quad i_c(\theta_r)=i_a\left(\theta_r+\frac{4\pi}{3N_P}\right); \quad (65,66)$$

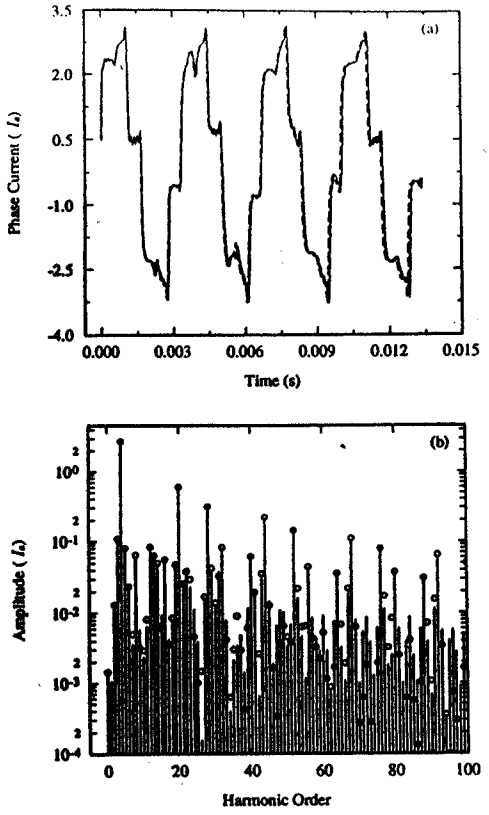

Fig. 4 Steady-state phase current of the NLTV model using the modified harmonic balance method; (a) time domain, (b) frequency domain. Key: solid line: the full model, dashed line and circles: the reduced model.

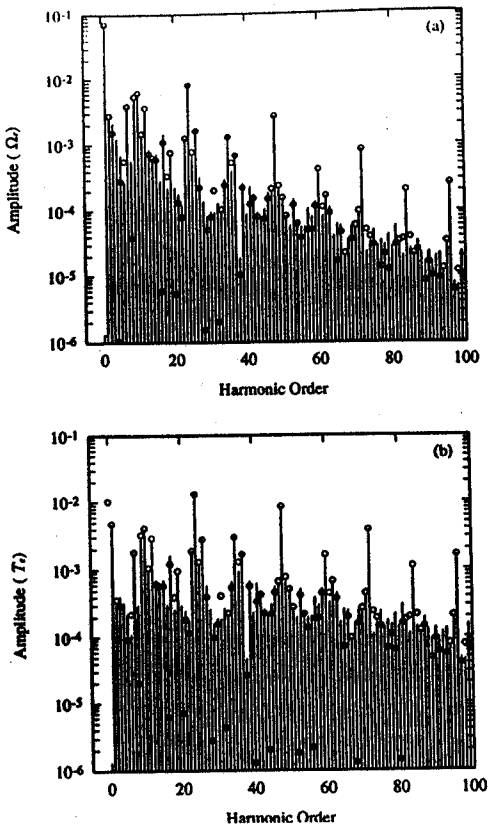

Fig. 5 Steady-state spectra of the NLTV model using the modified harmonic balance method; (a) rotor angular velocity, (b) torque. Key: solid line: the full model, circles: the reduced model.

The trigonometric collocation matrix of phase b, $\mathbf{T}_b$, with respect to the Fourier coefficients of phase a is given by

$$T_{bi,1} = 1 \quad T_{bi,2j-1} = \sin\left[f_j\left(\theta_{r,i} - \frac{4\pi}{3N_p}\right)\right];$$

$$T_{bi,2j} = \cos\left[f_j\left(\theta_{r,i} - \frac{4\pi}{3N_p}\right)\right]$$

$$\theta_{r,i} = \frac{2\pi(i-1)}{M}; \quad i = 1, \ldots, M; \quad j = 1, \ldots, N \quad (67a\text{–}d)$$

The collocation matrix $\mathbf{T}_c$ for phase c is obtained by substituting $-4\pi/3N_P$ with $+4\pi/3N_P$ in the above equation. Similarly, the collocation matrices for the derivative of phase currents $\mathbf{T}_{v,b}$ and $\mathbf{T}_{v,c}$ are defined. Following the procedure used in the previous section, the Jacobian matrix is derived.

$$\mathbf{J} = \begin{bmatrix} \mathbf{J}^{ii} & \mathbf{J}^{i\Omega} \\ \mathbf{J}^{\Omega i} & \mathbf{J}^{\Omega\Omega} \end{bmatrix}$$

$$\mathbf{J}^{ii} = \{\mathbf{T}^T\mathbf{T}\}^{-1}\mathbf{T}^T\{\sum_{i=a,b,c} \mathbf{Q}_{ai}^1\mathbf{T}_i + \mathbf{Q}_{ai}^2\mathbf{T}_{v,i}\}$$

$$\mathbf{J}^{i\Omega} = \{\mathbf{T}^T\mathbf{T}\}^{-1}\mathbf{T}^T\mathbf{Q}_a^3\mathbf{T}$$

$$\mathbf{J}^{\Omega i} = \{\mathbf{T}^T\mathbf{T}\}^{-1}\mathbf{T}^T\{\sum_{i=a,b,c} \mathbf{Q}_i^4\mathbf{T}_i\}$$

$$\mathbf{J}^{\Omega\Omega} = \{\mathbf{T}^T\mathbf{T}\}^{-1}\mathbf{T}^T\{\mathbf{Q}^5\mathbf{T} + \mathbf{Q}^6\mathbf{T}_v\} \quad (68a\text{–}e)$$

The computing time of the full NLTV model is about three times that of the reduced model for this case. Comparisons of the full and reduced NLTV models are shown in Figs. 4 and 5. Excellent agreement is obvious for most of the harmonics. Also, from Table 2 it is clear that there is little difference in $\bar{\Omega}_r$ between the full and reduced order NLTV models. Therefore, when the reduced model is employed, no significant loss of accuracy occurs but a considerable improvement in computational efficiency is achieved.

6 Linear Time-Varying (LTV) Model

Assuming that $\Omega_r(t) \approx \bar{\Omega}_r$, the mechanical system dynamics can be decoupled from the equivalent electrical circuits. Consequently, we need to apply the modified harmonic balance method only to the equivalent electrical circuits of Eq. (13). The governing equations are then simplified to

$$\bar{\Omega}_r\mathbf{L}(\theta_r)\mathbf{I}'(\theta_r) + \{\bar{\Omega}_r\mathbf{L}'(\theta_r) + \mathbf{R}\}\mathbf{I}(\theta_r) = \mathbf{V}(\theta_r) - \bar{\Omega}_r\hat{\mathbf{E}}(\theta_r) \quad (69)$$

By applying the procedure developed in the earlier sections, one obtains the following Jacobian matrix

$$\mathbf{J} = \begin{bmatrix} \mathbf{J}^{aa} & \mathbf{J}^{ab} & \mathbf{J}^{ac} \\ \mathbf{J}^{ba} & \mathbf{J}^{bb} & \mathbf{J}^{bc} \\ \mathbf{J}^{ca} & \mathbf{J}^{cb} & \mathbf{J}^{cc} \end{bmatrix}$$

$$\mathbf{J}^{ij} = \{\mathbf{T}^T\mathbf{T}\}^{-1}\mathbf{T}^T\{\mathbf{Q}_{ij}^1\mathbf{T}_v + \mathbf{Q}_{ij}^2\mathbf{T}\}; \; i, j = a, b, c \quad (70a, b)$$

Since this formulation is linear, the Jacobian is independent of the state variables (phase currents) and hence it needs to be evaluated only once during the entire process of iteration. The results of Figs. 6 and 7, as obtained from the harmonic balance scheme match well with those from numerical integration. Also by comparing the LTV and NLTV models, one observes that while the harmonic amplitudes of the phase currents have no significant differences, the harmonic amplitudes of the torque do show noticeable differences.

Similar to the reduced NLTV model, the LTV model can be further reduced to a single equation.

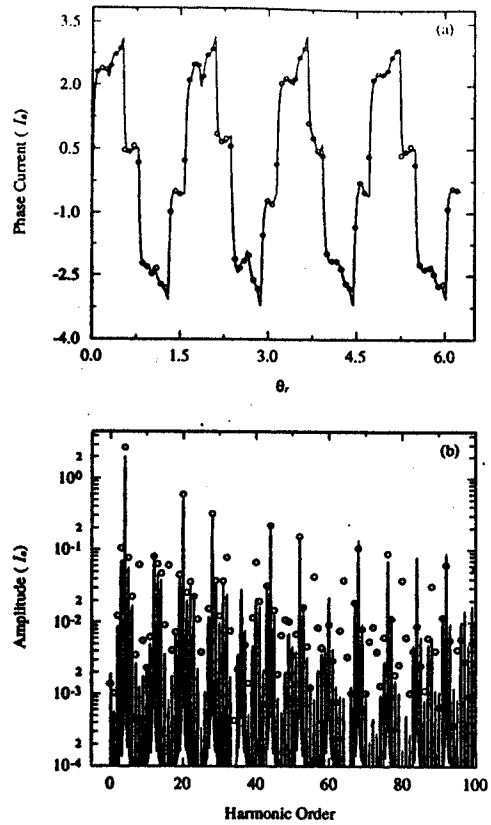

Fig. 6 Comparison of the steady-state phase current of the LTV model; (a) time domain, (b) frequency domain. Key: solid line: the numerical integration; dashed line and circles: the harmonic balance method.

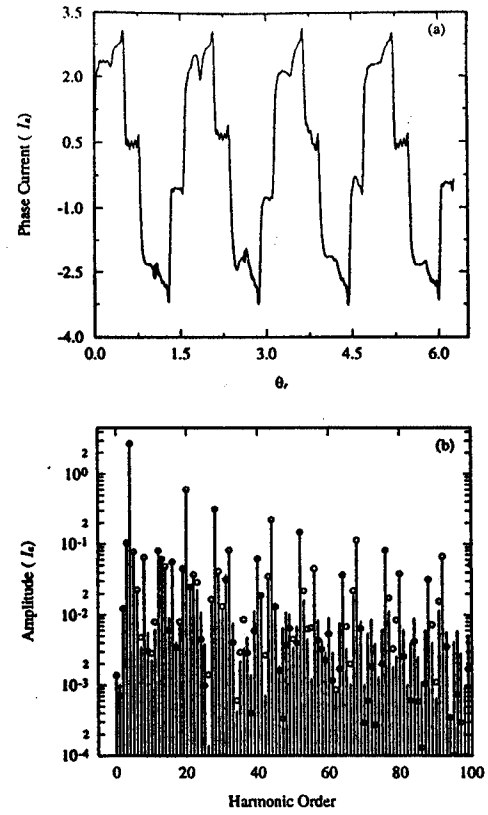

Fig. 8 Comparison of the steady-state phase current of the LTV model using the modified harmonic balance method; (a) time domain, (b) frequency domain. Key: solid line: the full model, dashed line and circles: the reduced model.

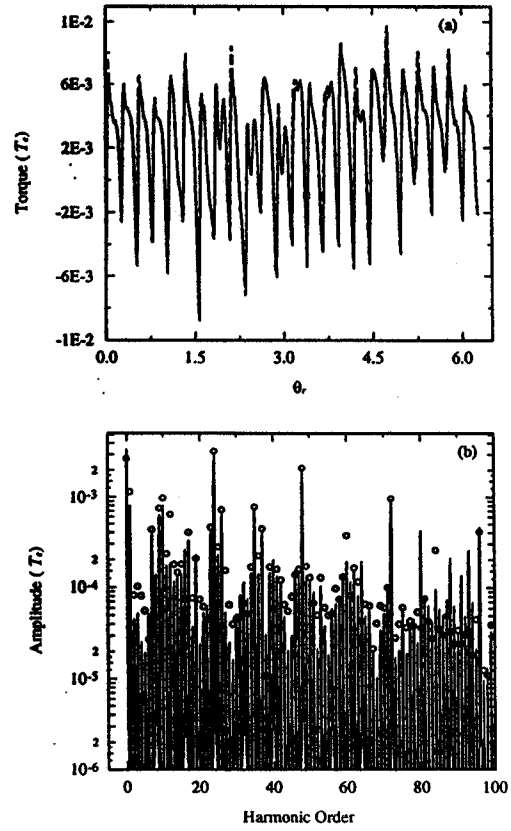

Fig. 7 Comparison of the steady-state torque of the LTV model; (a) time domain, (b) frequency domain. Key: solid line: the numerical integration; dashed line and circles: the modified harmonic balance method.

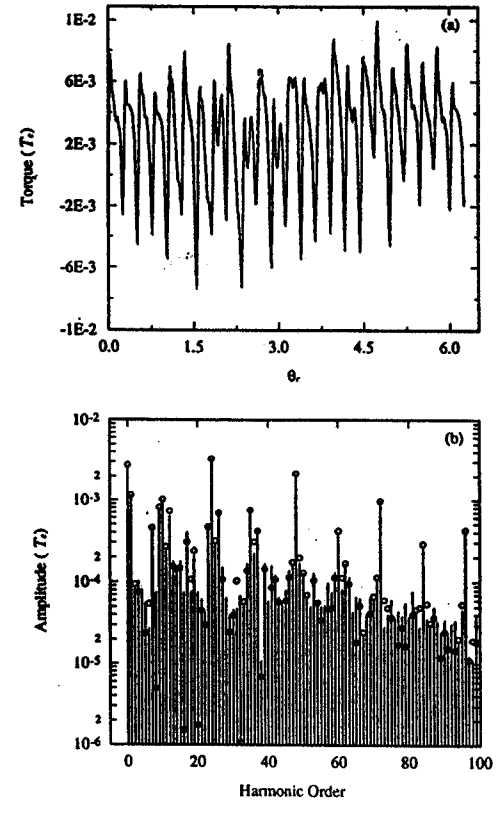

Fig. 9 Comparison of the steady-state torque of the LTV model using the modified harmonic balance method; (a) time domain, (b) frequency domain. Key: solid line: the full model, dashed line and circles: the reduced model.

$$(\bar{\Omega}_r L'_{aa} + R) i_a + \bar{\Omega}_r (L'_{ab} i_b + L'_{ac} i_c + i'_a L_{aa} + i'_b L_{ab} + i'_c L_{ac}) = v_a - \bar{\Omega}_r \hat{e}_a \quad (71)$$

Following the same approach demonstrated in developing the Jacobian matrix for the reduced NLTV model, the Jacobian matrix for the reduced LTV model is found as

$$\mathbf{J} = \{\mathbf{T}^T\mathbf{T}\}^{-1}\mathbf{T}^T\{\sum_{s=a,b,c} \mathbf{Q}^1_{ss}\mathbf{T}_{v,s} + \mathbf{Q}^2_{ss}\mathbf{T}_s\} \quad (72)$$

Comparisons between full and reduced LTV models are shown in Figs. 8 and 9. Again, a good agreement between the two models is evident, especially at the dominant harmonics.

7 Conclusion

This paper develops a new semi-analytical approach for the solution of a non-linear time-varying model of the BDCM. The transformation of the governing equations from a dual-domain to the spatial domain, thus exploiting the inherent spatial periodicity of the BDCM, is one of the major contributions of this study. This enables the rotor angular velocity fluctuation to be incorporated in the formulation as an unknown Fourier series, leading to the determination of mean operating speed and its harmonics together with the harmonics of the motor torque pulsations. This capability is a unique feature of the proposed modified harmonic balance method when compared with other conventional harmonic balance methods applied usually to simple non-linear systems. Further, unlike prior frequency domain analyses, complex effects such as dynamic eccentricity, open stator slots and magnetic saturation, have been included in the calculation of the motor torque Fourier coefficients. The modified harmonic balance method matches very well with the direct numerical integration over a wide range of frequencies. The proposed methodology has also been used to study a reduced order BDCM model which employs a balanced phase relationship among the phase current wave forms. Our method significantly reduces the dimension of the Jacobian matrix, and consequently the computing time with no significant loss of accuracy. The methodology presented here can be easily extended to other complex dynamic systems such as gear drives.

Acknowledgment

The authors gratefully acknowledge the IBM Corporation for sponsoring this research and the Graduate School of The Ohio State University for awarding a fellowship to the first author. The second and third authors also acknowledge the partial support from the Army Research Office (URI Grant DAAL-03-92-G-0120; Project Monitor: Dr. T. L. Doligalski) which enabled them to develop the methodology.

References

Bolton, H. R., and Ashen, R. A., 1984, "Influence of Motor Design and Feed-Current Waveform on Torque Ripple in Brushless D.C. Drives," *IEE Proceeding-B Electric Power Applications*, Vol. 131, No. 3, pp. 82–90.

Bolton, H. R., Liu, Y. D., and Mallinson, N. M., 1986, "Investigation into a Class of Brushless DC Motor with Quasisquare Voltages and Currents," *IEE Proceedings-B Electric Power Applications*, Vol. 133, No. 2, pp. 103–111.

Boules, N., 1985, "Prediction of No-Load Flux Density Distribution in Permanent Magnet Machines," *IEEE Transactions on Industry Applications*, Vol. IA-21, pp. 633–643.

Cameron, J. R., Thomson, W. T., and Dow, A. B., 1986, "Vibration and Current Monitoring for Detecting Airgap Eccentricity in Large Induction Motors," *IEE Proceedings-B Electric Power Applications*, Vol. 133, No. 3, pp. 155–163.

Chua, L. O., and Ushida, A., 1981, "Algorithms for Computing Almost Periodic Steady-State Response of Nonlinear Systems to Multiple Input Frequencies," *IEEE Transactions on Circuits and Systems*, Vol. CAS-28, No. 10, pp. 953–971.

Jufer, M., 1987, "Brushless DC Motors—Gap Permeance and PM-MMF Distribution Analysis," *Proceedings—Sixteenth Annual Symposium, Incremental Motion Control Systems and Devices*, pp. 21–25.

Krause, P. C., and Wasynczuk, O., 1989, *Electromechanical Motion Devices*, McGraw-Hill, New York.

Lee, M.-R., and Singh, R., 1992, "Identification of Pure Tones Radiated by Brushless D.C. Motors Used in Computer Disk Drives," *Noise Control Engineering Journal*, Vol. 39, No. 2, pp. 67–75.

Ling, F. H., and Wu, X. X., 1987, "Fast Galerkin's Method and Its Application to Determine Periodic Solutions of Non-Linear Oscillators," *International Journal of Non-Linear Mechanics*, Vol. 22, No. 2, pp. 89–98.

Pillay, P., and Krishnan, R., 1989, "Modeling, Simulation, and Analysis of Permanent-Magnet Motor Drives, Part II: the Brushless D.C. Motor Drive," *IEEE Transactions on Industry Applications*, Vol. 25, No. 2, pp. 274–279.

Urabe, M., and Reiter, A., 1966, "Numerical Computation of Nonlinear Forced Oscillations by Galerkin's Procedure," *Journal of Mathematical Analysis and Applications*, Vol. 14, pp. 107–140.

Ushida, A., and Chua, L. O., 1984, "Frequency-Domain Analysis of Nonlinear Circuits Driven by Multi-Tone Signals," *IEEE Transactions on Circuits and Systems*, Vol. CAS-31, No. 9, pp. 766–779.

Yang, S. J., 1981, *Low Noise Electric Motors*, Oxford Science Publications, England.